Experimental and numerical studies of press-braked S690 high strength steel channel section beams

Lulu Zhang [a], Fangying Wang [a], Yating Liang [b], Ou Zhao [*a]

[a] School of Civil and Environmental Engineering, Nanyang Technological University, Singapore

[b] School of Engineering, University of Glasgow, Glasgow, UK

[*] Corresponding author, Email: ou.zhao@ntu.edu.sg

Abstract

The present paper describes an in-depth experimental and numerical investigation into the flexural responses and strengths of press-braked S690 high strength steel channel section beams bent about the minor principal axes in both the 'u' and 'n' orientations. The experimental study was performed on eight press-braked channel sections, and comprised twenty-four material flat and corner coupon tests, initial local geometric imperfection measurements, and twelve beam tests in the four-point bending configuration. This was followed by a complementary numerical modelling programme, where finite element models were firstly developed and validated against the test results and afterwards adopted for performing parametric studies to obtain an additional numerical data bank over a wide variety of cross-section geometric sizes. The acquired test and numerical data were then employed to evaluate the applicability of the Eurocode slenderness limits for welded and hot-rolled internal webs (in compression) and outstand flanges (in stress gradients) to their press-braked counterparts, revealing that the Eurocode slenderness limits can be safely extended to cover the classifications of plate elements and cross-sections of press-braked S690 high strength steel channel section beams. Evaluation of the accuracy of the cross-section flexural strengths

predicted from various design codes established in Europe, North America and Australia/New Zealand was also made, based on the test and numerical data. The results of the quantitative evaluation generally revealed that (i) all the examined design codes lead to overall conservative and scattered predicted cross-section flexural strengths for press-braked S690 high strength steel channel section beams, and (ii) the European code results in more precise design flexural strengths for beams with relatively stocky channel sections, but less accurate strength predictions for beams with relatively slender channel sections, compared to the North American and Australian/New Zealand standards.

Keywords: Beam tests; Design standards; Finite element modelling; Local buckling; Minor-axis bending; Press-braked channel sections; S690 high strength steel

1. Introduction

High strength steels (HSSs) are gaining increasing attention in the construction of long-span and high-rise structures subjected to heavy vertical loading, owing to their superior strength-to-weight ratios, allowing structural components to be designed with small cross-section dimensions and light weights. For example, press-braked high strength steel S690 U-shaped chords were used in the roof truss structure of the Friends Arena Stadium in Stokholm, Sweden, and cold-formed high strength steel S690 hollow sections were employed in the Nesenbach Valley Bridge in Stuttgart, Germany. Despite the great advantages of high strength steels over the conventional normal strength mild steels, the lack of efficient design rules and the high vulnerability to global instability have impeded the actual widespread application of high strength steels in construction engineering. Experimental studies have therefore been prompted to verify the structural performances of various types of high strength steel components and develop precise and efficient design methods. The focus of this paper is on the in-plane flexural behaviour and bending resistances of press-braked S690 high strength steel channel section beams, and previous relevant experimental studies are firstly briefly reviewed. Pham and Hancock [1] conducted twenty-four four-point bending tests on cold-formed high strength steel lipped channel sections about the major principal axes to study their local and distortional buckling responses and strengths. Lee et al. [2] carried out both four-point and three-point bending tests on HSB800 and HSA800 steel (with the nominal yield stresses of 800 MPa) I-section beams to examine their in-plane flexural behaviour, strengths and rotation capacities. Wang et al. [3] investigated the local stability and bending strengths of hot-rolled square and rectangular hollow sections fabricated from S460 and S690 high strength steels through twenty-two in-plane bending tests, whilst the structural responses of cold-formed high strength steel (with a range of nominal yield stresses from 700 MPa to 1100 MPa) tubular beams were experimentally examined by Ma et al. [4]. Jiao and Zhao [5] reported experimental studies on cold-formed circular hollow section beams made of high strength steel (with the nominal yield stress equal to 1350 MPa) and assessed the cross-section slenderness limits. The brief review revealed that although experimental investigations have been carried out on high strength steel open and tubular section beams in bending about their symmetric axes, there were no studies on high strength steel beam members bent about an axis that is not one of the symmetric axes.

This paper describes an experimental and numerical study of the in-plane flexural performance and strengths of press-braked S690 high strength steel channel section beams bent about the minor principal axes. The experimental study was performed on eight plain channel sections, and consisted of twenty-four tensile flat and corner coupon tests, initial local geometric imperfection measurements and twelve beam tests in the four-point bending configuration. This was complemented by a finite element (FE) modelling investigation, in which nonlinear

FE models were firstly developed and validated against the experimental observations and subsequently employed for carrying out parametric studies to derive an extended data bank over a broader spectrum of cross-section sizes. The test results and numerical data were compared with the flexural strengths predicted by the European code EN 1993-1-12 [6], North American specification AISI S100 [7] and Australian/New Zealand standard AS/NZS 4600 [8], allowing the accuracy of the established codified local buckling design provisions for press-braked S690 high strength steel channel section beams in minor-axis bending to be assessed.

2. Experimental study

2.1 General

For the purpose of addressing the lack of test data on press-braked S690 high strength steel channel section beams bent about the minor principal axes, a series of laboratory tests were firstly conducted. Eight plain channel sections (C 60×40×5, C 80×40×5, C 80×50×5, C 80×60×5, C 80×80×5, C 100×40×5, C 100×60×5 and C 120×40×5), press-braked from the same batch of hot-rolled grade S700MC high strength steel plates with the nominal material thickness of 5 mm, were adopted in the present experimental investigation. The identifier of each channel section is composed of a letter ‘C’ (indicating a channel section) and the nominal section dimensions in millimetres (outer web height h × outer flange width b × wall thickness t – see Fig. 1). Overall, the experimental programme included twenty-four tensile flat and corner coupon tests to determine the material characteristics of grade S690 high strength steel, initial local imperfection measurements to obtain the geometric deviations of the constituent plate elements of each beam specimen, and twelve four-point bending tests to acquire the flexural strengths of S690 high strength steel channel section beams bent about the minor principal axes and study their in-plane flexural behaviour.

2.2 Material tests

The channel section beam specimens studied in this paper were fabricated by press-braking, which induced high localised plastic strains at the corner regions, thus leading to an enhancement in material strength, though accompanied by a reduction in ductility. Material tensile flat and corner coupon tests were both conducted to obtain the stress–strain curves and key material characteristics of the considered press-braked S690 high strength steel channel sections. One flat coupon and one corner coupon were respectively cut along the centrelines of the flat part and corner region of each section in the longitudinal direction; moreover, additional sets of flat and corner coupons were also extracted from channel sections C 80×40×5, C 80×60×5, C 80×80×5 and C 100×40×5 for the purpose of carrying out repeated tests. All the flat and corner coupons were machined according to the geometric requirements given in ASTM E8/E8M-15a [9], with the widths of 12.5 mm and gauge lengths of 50 mm. Material tensile coupon tests were performed utilising an INSTRON 250 kN hydraulic testing machine under displacement control, with the initial loading rate of 0.05 mm/min before attainment of the nominal material yield stresses and a higher rate of 0.8 mm/min thereafter until failure of the coupons. Note that flat and V-shaped end clamps were respectively utilised for gripping flat and corner coupons during material testing. The material tensile coupon test setup [10–12] is displayed in Fig. 2, including two strain gauges attached to the mid-height of the coupon and an extensometer mounted onto the central necked portion of the coupon. The measured flat and corner material stress–strain curves of the eight considered press-braked S690 high strength steel plain channel sections are respectively presented in Figs. 3(a) and 3(b), with a summary of the key measured material properties reported in Table 1, in which E is the Young's modulus, f_y is the yield stress, f_u is the ultimate stress, f_u/f_y is the material ultimate-to-yield stress ratio, and ε_u and ε_f are respectively the strains at the ultimate stress and fracture. The corner coupons, as expected, exhibit higher material strengths but with reduced ductility, compared with their flat counterparts. It can be seen from Figs. 3(a) and (b) that both the flat and corner coupons display relatively rounded material responses with no obvious yield plateaus and sharply defined yield stresses, and the corresponding 0.2% proof stresses are therefore defined as the material yield stresses [13–15] in Table 1.

2.3 Measurements on initial local geometric imperfections

The in-plane flexural responses and strengths of beam members can be affected by their initial local geometric imperfections, which were therefore carefully measured for each S690 high strength steel channel section beam specimen prior to the bending tests. The procedure for initial local geometric imperfection measurements was in line with that reported by Schafer and Peköz [16], and the setup is depicted in Fig. 4, in which the beam specimen is mounted on the milling machine bed and two linear variable differential transducers (LVDTs) are fixed to the uniformly movable machine head, with the tips pointing at each constituent plate element of the channel section beam specimen to record the local deviations along two representative lines in the longitudinal direction. For each plate element, the measured data points from LVDTs were then fitted by a linear regression surface, with the initial local geometric imperfection amplitude taken as the largest derivation from the linear regression surface to the original measured data points [17–19], as reported in Table 2, where ω_w, ω_{f1} and ω_{f2} respectively denote the initial local geometric imperfection amplitudes of the internal web and two outstand flanges, whilst the initial local geometric imperfection amplitude of the beam specimen ω_0 is given as the maximum of ω_w, ω_{f1} and ω_{f2}.

2.4 Four-point bending tests

A total of twelve four-point bending tests were performed to study the in-plane flexural behaviour and resistances of press-braked S690 high strength steel channel section beams about the minor principal axes. Specifically, for each of the eight examined channel sections, one four-point bending test was performed about the minor principal axis in the 'n' orientation, which induces the maximum tensile stress in the flange tip – see Fig. 5(a), whilst additional four-point bending tests were also carried out on channel sections C 80×40×5, C 80×60×5, C 80×80×5 and C 100×40×5 in the 'u' orientation, which results in the maximum compressive stress in the flange tip – see Fig. 5(b). All the beam tests were performed by using an INSTRON 2000 kN hydraulic testing frame at a fixed loading rate of 1 mm/min. Fig. 6 displays the four-point bending test setup, in which the beam specimen is simply supported between two steel rollers while a spreader beam is utilised to transfer load at the third-points of the flexural span between the two steel rollers [20–23], underpinning bolts (inserted between the inner faces of the two flanges) are used together with G-clamps (clamped onto the outer faces of the flanges) at the two supports and two loading points for the purpose of precluding local bearing and crushing failure at these positions, and three line transducers are arranged below the channel section beam specimen to measure the vertical deflections at the mid-span and two loading points. The readings from the three line transducers were used to derive the curvature of the constant moment span between the loading points κ through Eq. (1) [24], where D_M and D_L are the measured vertical deflections at the mid-span and two loading points, respectively, and L_0 is length of the constant moment span. In the present testing programme, the nominal length of each beam specimen L was selected to be 1000 mm, and the flexural span between the two end steel rollers L_f was equal to 900 mm, leading to the length of the constant moment span L_0 of 300 mm; the resulting span-to-height ratios of the beam specimens fell between 10 and 25, ensuring that all the beam specimens fail by in-plane flexure with negligible influence from shear. Table 2 reports the measured geometric dimensions of each press-braked S690 high strength steel channel section beam specimen, in which r denotes the internal corner radius of the channel section. The beam specimen ID begins with the cross-section identifier and ends with a letter 'n' or 'u' (indicating the bending orientation).

$$\kappa = \frac{8\left(D_M - D_L\right)}{4\left(D_M - D_L\right)^2 + L_0^2} \tag{1}$$

The key results acquired from the four-point bending tests are presented in Table 3, where $M_{u,test}$ is the failure moment, κ_f is the curvature at the failure moment, and $M_{u,test}/M_{pl}$ and $M_{u,test}/M_{el}$ are respectively the ratios of the experimental failure moment to the cross-section plastic and elastic moment resistances, in which $M_{pl}=W_{pl}f_y$ and $M_{el}=W_{el}f_y$ are given as the products of the material yield stress and the plastic and elastic section moduli, respectively; note that W_{el} and W_{pl} are determined about the elastic neutral axis (ENA) and plastic neutral axis (PNA) along the minor principal axis direction – see Fig. 5. The moment–curvature curves for press-braked S690 high strength steel channel section beam specimens bent in the 'n' and 'u' orientations are plotted in Fig. 7(a) and 7(b), respectively. Note that channel section beams are more susceptible to local buckling for the cases of 'u'-orientation bending, and thus display steeper post-ultimate moment–curvature responses as well as lower failure moments and smaller curvatures at the failure moments than those obtained from the same channel section beams bent in the 'n' orientation. All the tested press-braked S690 high strength steel channel section beam specimens exhibited visible in-plane bending deformation, and more obvious local buckling failure was observed for those specimens bent in the ‘u’ orientation; typical deformed failure modes of the beam specimens C 80×60×5-n and C 80×60×5-u bent about the minor principal axes in the ‘n’ orientation and in the ‘u’ orientation are respectively shown in Figs. 8 and 9.

3. Numerical modelling

3.1 General

This section presents a parallel numerical modelling investigation into the flexural behaviour of press-braked S690 high strength steel channel section beams, carried out by nonlinear FE analysis package ABAQUS [25]. Development and validation of press-braked S690 high strength steel channel section beam FE models were firstly detailed in Sections 3.2, followed by parametric studies, which were performed based on the validated FE models to acquire an extended numerical data bank over a wider range of cross-section sizes.

3.2 Development and validation of FE models

The shell element S4R, having been extensively used by the authors in the numerical simulations of thin-walled steel open section structural members under various loading conditions [12,15,18–21,26,27], was adopted in the present finite element modelling of press-braked S690 high strength steel channel section beams. The mesh size was selected to be equal to the wall thickness t of the modelled channel section for the flat regions while a finer mesh of four elements was used to discretise the corner portions of the cross-section to capture the rounded geometric profiles, following a prior mesh sensitivity study taking into account both the numerical accuracy and computational efficiency. The measured flat and corner stress–strain curves were converted into the true stress–strain responses and then assigned to the flat regions and corners of the modelled channel section beams. For the ease of setting boundary conditions, the two cross-sections at the supports were respectively coupled to two reference points, which were positioned at the mid-point between the flange tips for the ‘n’-orientation bending cases and at the mid-point of the web for the ‘u’-orientation bending cases; to mimic the same simply-supported boundary condition adopted in the experiments, one reference point was allowed for rotation about the bending axis as well as longitudinal translation, whilst the other reference point was allowed only for rotation about the same bending axis. Besides, the cross-sections at the two loading points were respectively set as rigid planes, allowed to rotate about the bending axis and translate in both the vertical and longitudinal directions, in order to replicate the four-point bending configuration. The initial local geometric imperfections were also included in the FE models. The imperfection distribution profile of each beam model was assumed to be of the first elastic local buckling mode shape [19–21], representing the most unfavourable imperfection pattern of the beam model. Three imperfection amplitudes, including the measured value ω_0 and 1/10 and 1/100 of the measured wall thickness of the channel section, were utilised to factor the imperfection distribution profile of each beam FE model, with the aim of assessing the sensitivity of the developed beam FE models to local imperfection amplitudes. Upon development of the press-braked S690 high strength steel channel section beam FE models, nonlinear static analyses were conducted by applying vertical displacements at the locations of the two loading points to simulate the same loading procedure and scheme adopted in the experiments.

The numerically derived results, including the ultimate moments, moment–curvature histories and deformed failure modes, were then compared with the experimental observations to verify the accuracy of the developed beam FE models. Table 4 lists the FE to experimental ultimate moment ratios for the three examined imperfection amplitudes. The results of the comparisons indicated that all the three imperfection amplitudes lead to overall accurate predictions of the test ultimate moments, whilst the imperfection value of 1/100 of the wall thickness yields the best agreement between the experimental and FE ultimate moments. Figs. 10 and 11 present comparisons of the moment–curvature curves obtained from tests with those from nonlinear FE analyses for typical S690 high strength steel channel section beam specimens C 80×60×5-n and C 80×60×5-u bent about the minor principal axes in the 'n' orientation and in the 'u' orientation, respectively, both indicating that the test moment–curvature histories are well represented by the corresponding numerically derived responses. The deformed failure modes displayed by the beam specimens C 80×60×5-n and C 80×60×5-u were also shown to be successfully captured by their numerical counterparts, as depicted in Figs. 8 and 9. Therefore, the beam FE models, developed based on the aforementioned modelling assumptions, are capable of simulating the in-plane flexural behaviour of the test press-braked S690 high strength steel channel section beam specimens, and deemed to be validated.

3.3 Parametric studies

In this section, the validated FE models were utilised to perform parametric studies for the purpose of generating an additional numerical data bank on press-braked S690 high strength steel channel section beams over a broad range of cross-section geometric sizes. Table 5 summarises the cross-section dimensions selected for the present parametric studies. Five cross-section web-to-flange aspect ratios of 1.0, 1.5, 2.0, 2.5 and 3.0 were considered in the present parametric studies through fixing the outer web heights of the modelled channel sections at 150 mm and setting the flange widths to be respectively equal to 150 mm, 100 mm, 75 mm, 60 mm and 50 mm. In addition, the selected wall thicknesses fell between 2.8 mm and 24 mm, leading to a broad range of non-slender and slender channel sections being considered. The flexural spans of the beam models were kept constant as 900 mm, with the two loading points located at the third-points of the flexural spans. With regards to the modelling of material and imperfections, the measured flat and corner stress–strain curves of channel section C 80×60×5 were adopted throughout the present parametric studies, whilst the imperfection distribution pattern of each beam model was assumed to be of the first elastic local buckling mode shape, with the maximum imperfection amplitude equal to 1/100 of the wall thickness. A total of 118 press-braked S690 high strength steel channel section beams bent about the minor principal axes in both the 'n' and 'u' orientations were modelled.

4. Evaluation of existing design standards

4.1 European code EN 1993-1-12 (EC3)

4.1.1. General

The current EN 1993-1-12 [6] for high strength steel structures with material grades up to S690 was developed in line with the corresponding EN 1993-1-1 [28] for normal strength mild steels. Regarding the design of beam members susceptible to in-plane failure, both EN 1993-1-1 [28] and EN 1993-1-12 [6] adopt the framework of cross-section classification, i.e. the flexural strength of a cross-section is dependent on its class. Four cross-section classes were prescribed in the current Eurocodes [6,28]: Class 1 and Class 2 sections, also termed plastic sections, are capable of reaching the plastic moment capacities M_{pl} at failure; Class 3 sections, also known as elastic sections, are able to develop their elastic moment capacities M_{el} at failure; Class 4 (slender) sections fail before the yield stresses are attained due to premature local buckling in the slender plate elements, with the cross-section flexural strengths limited to the effective moment capacities M_{eff}. Classification of a cross-section is made according to the class of its most slender constituent plate element, whilst each constituent plate element within the cross-section is categorised by comparing its flat width-to-thickness ratio (c/t) with the specified slenderness limits, in which $c=b-t-r$ for outstand flanges and $c=h-2t-2r$ for internal webs. It is worth noting that the existing European codes EN 1993-1-1 [28] and EN 1993-1-12 [6] only provide slenderness limits for classification of hot-rolled and welded plate elements and cross-sections, with no guidelines on their cold-formed (press-braked) counterparts. Evaluation on the applicability of the Eurocode Class 2 and Class 3 slenderness limits to press-braked S690 high strength steel channel sections in bending is firstly made in Section 4.1.2, followed by assessment of the Eurocode cross-section flexural strength predictions in Section 4.1.3.

4.1.2 Class 2 and Class 3 slenderness limits

The applicability of the EC3 Class 2 and Class 3 slenderness limits for outstand flanges under stress gradients and with tips in compression was evaluated, based on the failure moments obtained from tests and parametric studies on press-braked S690 high strength steel channel section beams bent about the minor principal axes in the 'u' orientation. The graphic evaluation results are shown in Figs. 12 and 13, respectively, in which the failure moments are respectively normalised by the cross-section plastic and elastic moment capacities, and then plotted against the $\alpha c/(t\varepsilon)$ and $c/(t\varepsilon k_\sigma^{0.5})$ ratios of the flanges, together with the corresponding EC3 Class 2 slenderness limit ($\alpha c/(t\varepsilon)=10$) and Class 3 slenderness limit ($c/(t\varepsilon k_\sigma^{0.5})=21$) for outstand flanges under stress gradients and with tips in compression, where $\varepsilon=(235/f_y)^{0.5}$ is a material parameter, α is the ratio of the width of the compressive portion of the flange to the flat width of the flange, and k_σ is the plate buckling coefficient and equal to $0.57 - 0.21\psi + 0.07\psi^2$ for outstand flanges under stress gradients and with tips in compression [29], in which ψ is the end tensile to compressive stress ratio of the flat part of the flange. It was generally found from Fig. 12 that the test and FE data points intersect with the unity line at the $\alpha c/(t\varepsilon)$ ratio of around 10 and are accurately captured by the current Eurocode Class 2 slenderness limit ($\alpha c/(t\varepsilon)$=10). However, the test and FE data, depicted in Fig. 13, intersect with the unity line at the $c/(t\varepsilon k_\sigma^{0.5})$ ratio of around 38, revealing that the current Eurocode Class 3 slenderness limit ($c/(t\varepsilon k_\sigma^{0.5})$=21) is excessively conservative. In sum, the results of the evaluation indicate that the current Eurocode Class 2 slenderness limit ($\alpha c/(t\varepsilon)$=10) can be safely and accurately used for the classification of the outstand flanges of press-braked S690 channel sections bent about the minor principal axes in the 'u' orientation, while the Class 3 slenderness limit ($c/(t\varepsilon k_\sigma^{0.5})$=21) is excessively conservative.

On the basis of the experimental and numerical data on S690 high strength steel channel section beams bent about the minor principal axes in the 'n' orientation, the applicability of the Eurocode Class 2 and Class 3 slenderness limits for internal plate elements in compression were also evaluated. Figs. 14 and 15 present the normalised experimental and numerical ultimate moments (by the cross-section plastic and elastic moment capacities, respectively) plotted against the web flat width-to-thickness ratios $c/(t\varepsilon)$, together with the Eurocode Class 2 and Class 3 slenderness limits ($c/(t\varepsilon)$=38 and $c/(t\varepsilon)$=42) for internal plate elements in compression. Similar conclusions can be made that the EC3 Class 2 slenderness limit ($c/(t\varepsilon)$=38) for internal plate elements in compression is capable of precisely differentiating Class 1 and Class 2 internal webs of press-braked S690 high strength steel channel sections from their Class 3 counterparts, while the Class 3 slenderness limit ($c/(t\varepsilon)$=42) leads to safe but rather uneconomic classification results.

4.1.3 Cross-section flexural strength predictions

In this section, the EC3 cross-section flexural strength predictions of press-braked S690 high strength steel channel section beams bent about the minor principal axes in both the 'n' and 'u' orientations were evaluated through comparisons against the acquired test and numerical failure moments. The design cross-section flexural strengths, as specified in EN 1993-1-12 [6], are given as the plastic (M_{pl}=$W_{pl}f_y$), elastic (M_{el}=$W_{el}f_y$) and effective (M_{eff}=$W_{eff}f_y$) moment capacities for Class 1 (or Class 2), Class 3 and Class 4 channel sections, respectively, in which W_{eff} is the effective section modulus and determined based on the effective cross-section area excluding the ineffective area due to local buckling. The effective area of each constituent plate element of the channel section consists of (i) the full area of the tensile portion and (ii) the effective area of the compressive portion, calculated as the product of the wall thickness t and the effective width of the compressive portion b_{eff}=ρb_c, in which b_c is equal to the full width of the compressive portion of the plate element and ρ is the reduction factor (accounting for loss of effectiveness of the compressive portion of the plate element due to local buckling), with the formulae shown by Eqs. (2) and (3) for outstand flanges and internal webs, respectively, in which $\overline{\lambda}_p$ is the plate element slenderness and determined as $\sqrt{f_y / f_{cr}}$, where f_{cr} is the elastic local buckling stress of the plate element, as given by Eq. (4); note that the plate buckling coefficient k_σ is equal to 4.0 for internal webs in pure compression, but taken as 0.57 – 0.21ψ + 0.07ψ^2 for outstand flanges under stress gradients and with tips in compression [29]. Upon calculation of the effective areas of all the slender plate elements of the Class 4 channel section in bending, the effective section modulus W_{eff} can then be derived; it is worth noting that cumbersome iterations may be involved in the calculation of W_{eff} due to the shift in effective neutral axis along with each round of calculation.

$$\rho = \frac{1}{\bar{\lambda}_p} - \frac{0.188}{\bar{\lambda}_p^{\ 2}} \leq 1.0 \quad \text{for } \bar{\lambda}_p > 0.748 \tag{2}$$

$$\rho = \frac{1}{\bar{\lambda}_p} - \frac{0.055(3+\psi)}{\bar{\lambda}_p^{\ 2}} \leq 1.0 \quad \text{for } \bar{\lambda}_p > 0.673 \tag{3}$$

$$f_{cr} = \frac{k_\sigma \pi^2 E}{12(1-\upsilon^2)} (\frac{t}{c})^2 \tag{4}$$

The mean ratios of the experimental (and numerical) failure moments M_u to the flexural strengths predicted by EN 1993-1-12 [6] $M_{u,EC3}$ are reported in Table 6(a). The mean $M_u/M_{u,EC3}$ ratios are respectively equal to 1.04, 1.79 and 1.78 for Class 1 (or Class 2), Class 3 and Class 4 press-braked S690 high strength steel channel section beams bent in the 'n' orientation, with the coefficients of variation (COVs) of 0.03, 0.02 and 0.03, while the mean ratios of $M_u/M_{u,EC3}$ are equal to 1.12, 1.82 and 2.00 for those Class 1 (or Class 2), Class 3 and Class 4 channel section beams bent in the 'u' orientation, respectively, with the COVs of 0.06, 0.04 and 0.08. The results of the quantitative assessment revealed that the existing EN 1993-1-12 [6] generally yields relatively accurate flexural strength predictions for Class 1 and Class 2 press-braked S690 high strength steel channel section beams in minor-axis bending, but results in excessively conservative design flexural strengths for their Class 3 and Class 4 counterparts, and that the EC3 flexural strength predictions are more conservative and scattered for the cases of 'u'-orientation bending than for the cases of 'n'-orientation bending. This is also evident in Figs. 16(a) and 16(b), where the failure moments for channel section beams bent in the 'n' and 'u' orientations, normalised by the design flexural strength predictions, are plotted against the flat width-to-thickness ratios of the webs and flanges, respectively.

4.2 North American Specification AISI S100 and Australian/New Zealand Standard AS/NZS 4600

The North American specification AISI S100 [7] and Australian/New Zealand standard AS/NZS 4600 [8] were established specifically for cold-formed steel members with material grades up to S690. Regarding the design of flexural members, both standards adopt the same provisions that the bending moment capacities shall be taken as the minimum of the local buckling, lateral-torsional buckling and distortional buckling strengths. The present study is focusing on S690 high strength steel channel section beams in bending about the minor principal axes, which fail by in-plane local buckling, without any out-of-plane lateral-torsional buckling and distortional buckling. Therefore, the bending moment capacities of the studied S690 high strength steel channel section beams M_{nl} were calculated as the corresponding local buckling strengths. Both AISI S100 [7] and AS/NZS 4600 [8] specify that the design bending moment capacities shall be calculated based on either initiation of yielding or inelastic reserve capacities, with the first approach adopted herein. Specifically, the elastic and effective moment capacities (M_{el}=$W_{el}f_y$ and M_{eff}=$W_{eff}f_y$) were taken as the design bending moment capacities for non-slender and slender sections, respectively. Regarding calculation of the effective section modulus W_{eff}, AISI S100 [7] and AS/NZS 4600 [8] adopt the same procedure as that employed in EN 1993-1-12 [6], but with different reduction factor expressions for internal webs and outstand flanges, as given by Eqs. (5) and (6), respectively,

$$\rho = \frac{1}{\lambda} - \frac{0.22}{\lambda^2} \le 1.0 \quad \text{for } \lambda > 0.673 \tag{5}$$

$$\rho = \frac{0.925}{\sqrt{\lambda}} \le 1.0 \quad \text{for } \lambda > 0.856 \tag{6}$$

in which $\lambda = \sqrt{f / f_{cr}}$ is the plate element slenderness, where f is the maximum compressive stress in the considered plate element and derived based on an assumption that the design stress distribution across the plate element is linear with the yield stress at the initial yielding point; note that f is less than f_y for the internal webs of channel sections bent in the 'n' orientation and thus the determined AISI (or AS/NZS) plate element slendernesses $\lambda = \sqrt{f / f_{cr}}$ are less than the corresponding EC3 plate element slendernesses $\bar{\lambda}_p = \sqrt{f_y / f_{cr}}$, and f_{cr} is determined from Eq. (4), of which the plate buckling coefficient k_σ for outstand flanges under stress gradients and with tips in compression is determined by an alternative expression prescribed in AISI S100 [7] and AS/NZS 4600 [8], as given by Eq. (7); note that the resulting AISI (or AS/NZS) plate element slendernesses $\lambda = \sqrt{f / f_{cr}}$ are also smaller than the EC3 plate element slendernesses $\bar{\lambda}_p = \sqrt{f_y / f_{cr}}$ for the outstand flanges of channel sections bent in the 'u' orientation.

$$k_\sigma = 0.145(b/h) + 1.256 \quad \text{for } 0.1 \leq b/h \leq 1.0 \tag{7}$$

Quantitative and graphic comparisons of the design cross-section bending moment capacities $M_{u,AISI}$ (or $M_{u,AS/NZS}$) with the test and numerical failure moments M_u were conducted and presented in Table 6(b) and Fig. 17, respectively. The mean ratios of $M_u/M_{u,AISI}$ (or $M_u/M_{u,AS/NZS}$) are equal to 1.85 and 1.66, with the COVs of 0.05 and 0.03, for non-slender and slender press-braked S690 high strength steel channel section beams bent in the 'n' orientation, respectively, while the $M_u/M_{u,AISI}$ (or $M_u/M_{u,AS/NZS}$) ratios are equal to 1.77 and 1.09, with the corresponding COVs of 0.17 and 0.06, for those non-slender and slender channel section beams in 'u'-orientation bending, respectively. Compared to EN 1993-1-12 [6], AISI S100 [7] and AS/NZS 4600 [8] were shown to yield excessively more conservative cross-section flexural strength predictions for non-slender S690 high strength steel channel section beams, owing to the lack of due consideration of plasticity, but more accurate and consistent cross-section flexural strength predictions for slender S690 high strength steel channel section beams, attributed mainly to the adoption of more relaxed (i.e. smaller) plate element slendernesses and more accurate plate element width reduction factors.

Evaluation of the codified design cross-section bending moment capacities was also carried out, based on the S690 high strength steel channel section beam test results only. Table 3 reports the experimental to predicted failure moment ratios $M_{u,test}/M_{u,pred}$ for each tested beam specimen. EN 1993-1-12 [6] was found to result in an overall higher level of design accuracy but lower degree of design consistency than AISI S100 [7] and AS/NZS 4600 [8].

5. Conclusions

A thorough testing and numerical modelling programme has been conducted to study the in-plane bending behaviour and capacities of press-braked S690 high strength steel channel section beams. The testing programme was carried out on eight channel sections, and involved twenty-four material flat and corner coupon tests, initial local geometric imperfection measurements and twelve beam tests bent about the cross-section minor principal axes in both the ‘u’ and ‘n’ orientations, while the numerical modelling programme included a simulation study to replicate the structural responses of the tested beams and a parametric study to generate an extended data bank over a wide variety of cross-section geometric sizes. The test and numerical results were firstly employed to assess the applicability of the Eurocode Class 2 and Class 3 slenderness limits for welded and hot-rolled outstand and internal plate elements to their cold-formed (press-braked) counterparts, indicating that the Eurocode slenderness limits can be safely used to perform classifications of plate elements and cross-sections of press-braked S690 high strength steel channel section beams. On the basis of the test and numerical results, the accuracy of the design cross-section bending moment capacities obtained from EN 1993-1-12 [6], AISI S100 [7] and AS/NZS 4600 [8] was then evaluated. The evaluation results generally revealed that (i) EN 1993-1-12 [6] yields accurate and consistent cross-section bending moment capacity predictions for stocky (Class 1 and Class 2) S690 high strength steel channel section beams, but conservative and scattered design cross-section bending moment capacities for their non-stocky (Class 3 and Class 4) counterparts, and (ii) AISI S100 [7] and AS/NZS 4600 [8] were shown to result in more conservative bending moment capacity predictions for non-slender S690 high strength steel channel section beams than EN 1993-1-12 [6], owing to the lack of due consideration of plasticity, but more accurate and consistent design bending moment capacities for relatively slender S690 high strength steel channel section beams, due to the adoption of more accurate effective width method.

Acknowledgements

The authors thank SSAB Swedish Steel Pte Ltd, Singapore for the assistance in fabricating press-braked S690 high strength steel channel section beams. Miss Liu Chang also provided help in the laboratory tests as part of her undergraduate final year project.

References

[1] Pham C H, Hancock G J. Experimental investigation and direct strength design of high-strength, complex C-sections in pure bending. Journal of Structural Engineering, 2013, 139(11): 1842-1852.

[2] Lee C H, Han K H, Uang C M, et al. Flexural strength and rotation capacity of I-shaped beams fabricated from 800-MPa steel. Journal of Structural Engineering, 2012, 139(6): 1043-1058.

[3] Wang J, Afshan S, Gkantou M, et al. Flexural behaviour of hot-finished high strength steel square and rectangular hollow sections. Journal of Constructional Steel Research, 2016, 121: 97-109.

[4] Ma J L, Chan T M, Young B. Experimental investigation of cold-formed high strength steel tubular beams. Engineering Structures, 2016, 126: 200-209.

[5] Jiao H, Zhao X L. Section slenderness limits of very high strength circular steel tubes in bending. Thin-walled structures, 2004, 42(9): 1257-1271.

[6] EN 1993-1-12. Eurocode 3: Design of steel structures – Part 1–12: Additional rules for the extension of EN 1993 up to steel grades S 700. Brussels (Belgium): CEN; 2007.

[7] AISI S100. North American specification for the design of cold-formed steel structural members. American Iron and Steel Institude; 2016.

[8] AS/NZS 4600. Cold-formed steel structures. Sydney: AS/NZS 4600:2005; 2005.

[9] American Society for Testing and Materials (ASTM). Standard test methods for tension testing of metallic materials. E8/E8M-15a. West Conshohocken, PA., USA: ASTM International; 2015.

[10] Huang Y, Young B. The art of coupon tests. Journal of Constructional Steel Research. 2014, 96: 159-175.

[11] Chen M T, Young B. Cross-sectional behavior of cold-formed steel semi-oval hollow sections. Engineering Structures, 2018, 177: 318-330.

[12] Sun Y, Liang Y, Zhao O. Testing, numerical modelling and design of S690 high strength steel welded I-section stub columns. Journal of Constructional Steel Research, 2019, 159: 521-533.

[13] Ma J L, Chan T M, Young B. Experimental investigation on stub-column behavior of cold-formed high-strength steel tubular sections. Journal of Structural Engineering (ASCE), 2015, 142(5): 04015174.

[14] Fang H, Chan T M, Young B. Material properties and residual stresses of octagonal high strength steel hollow sections. Journal of Constructional Steel Research, 2018, 148: 479-490.

[15] Zhang L, Wang F, Liang Y, Zhao O. Press-braked S690 high strength steel equal-leg angle and plain channel section stub columns: Testing, numerical simulation and design, Engineering Structures, 2019;201:109764.

[16] Schafer B, Peköz T. Computational modeling of cold-formed steel: characterizing geometric imperfections and residual stresses. Journal of Constructional Steel Research, 1998; 47(3): 193–210.

[17] Theofanous M, Liew A, Gardner L. Experimental study of stainless steel angles and channels in bending. Structures, 2015, 4: 80-90.

[18] Liang Y, Zhao O, Long Y, Gardner L. Stainless steel channel sections under combined compression and minor axis bending–Part 1: Experimental study and numerical modelling. Journal of Constructional Steel Research, 2019, 152: 154-161.

[19] Sun Y, Zhao O. Material response and local stability of high-chromium stainless steel welded I-sections. Engineering Structures, 2019, 178: 212-226.

[20] Sun Y, He A, Liang Y, Zhao O. In-plane bending behaviour and capacities of S690 high strength steel welded I-section beams. Journal of Constructional Steel Research, 2019;162:105741.

[21] Wang F, Zhao O, Young B. Flexural behaviour and strengths of press-braked S960 ultra-high strength steel channel section beams. Engineering Structures, 2019, 200: 109735.

[22] Arrayago I, Real E. Experimental study on ferritic stainless steel simply supported and continuous beams. Journal of Constructional Steel Research, 2016, 119: 50–62.

[23] Chen MT, Young B. Structural behavior of cold-formed steel semi-oval hollow section beams. Engineering Structures. 2019, 185: 400-411.

[24] Chan TM, Gardner L. Bending strength of hot-rolled elliptical hollow sections. Journal of Constructional Steel Research, 2008, 64(9): 971–986.

[25] Hibbitt, Karlsson & Sorensen, Inc. ABAQUS. ABAQUS/Standard user's manual volumes I-III and ABAQUS CAE manual. Version 6.12. Pawtucket (USA); 2012.

[26] Liang Y, Jeyapragasam V V K, Zhang L, Zhao O. Flexural-torsional buckling behaviour of fixed-ended hot-rolled austenitic stainless steel equal-leg angle section columns. Journal of Constructional Steel Research, 2019, 154: 43-54.

[27] Zhang L, Tan K H, Zhao O. Experimental and numerical studies of fixed-ended cold-formed stainless steel equal-leg angle section columns. Engineering Structures, 2019, 184: 134-144.

[28] EN 1993-1-1. Eurocode 3: Design of steel structures – Part 1–1: General rules and rules for buildings. Brussels (Belgium): CEN; 2005.

[29] EN 1993-1-5. Eurocode 3: Design of steel structures – Part 1–5: Plated structural elements. Brussels: European Committee for Standardization (CEN); 2015.

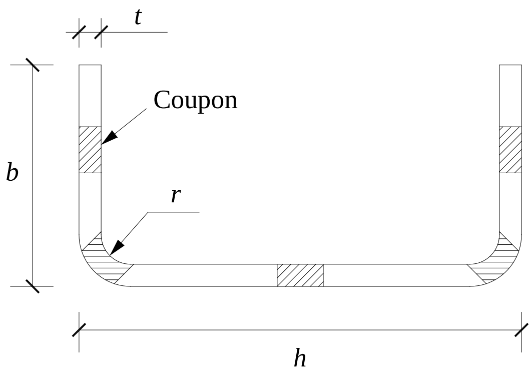

Fig. 1. Notation and locations of coupons.

Fig. 2. Tensile coupon test setup.

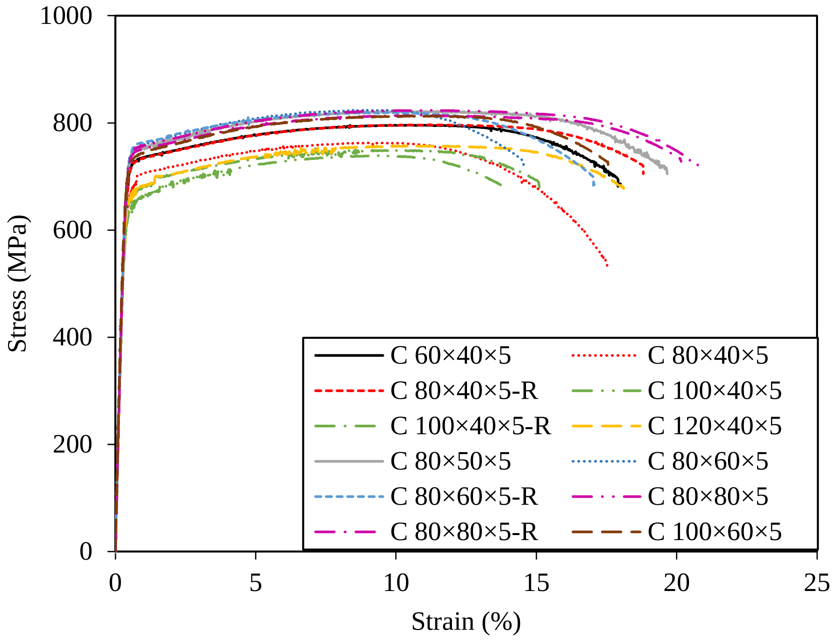

(a) Flat coupons

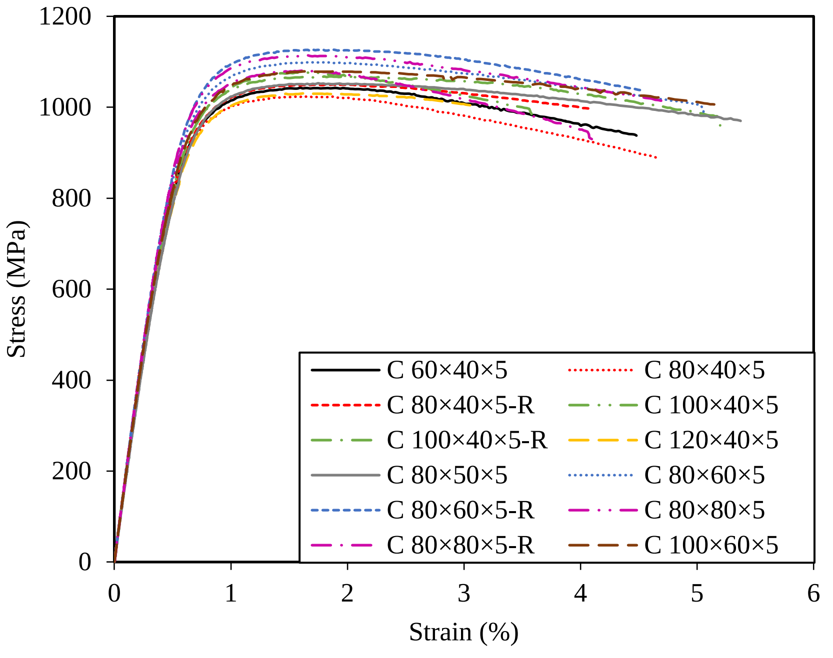

(b) Corner coupons

Fig. 3. Stress–strain curves measured from material tensile coupon tests on press-braked S690 high strength steel channel sections.

Fig. 4. Test setups for initial local geometric imperfection measurements.

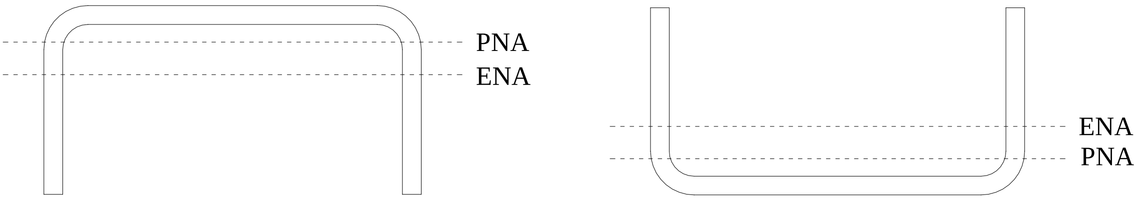

(a) Channel section bent in the 'n' orientation

(b) Channel section bent in the 'u' orientation

Fig. 5. Elastic neutral axes, plastic neutral axes and bending orientations for channel sections bent about the minor principal axes.

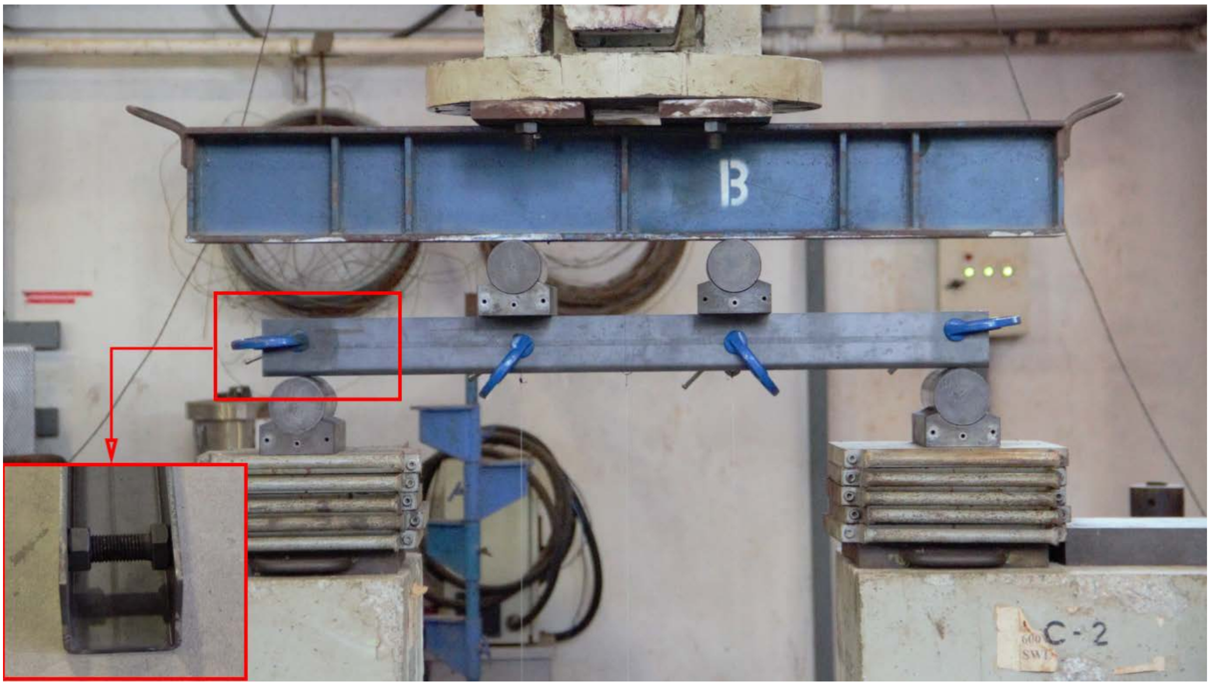

(a) Experimental setup

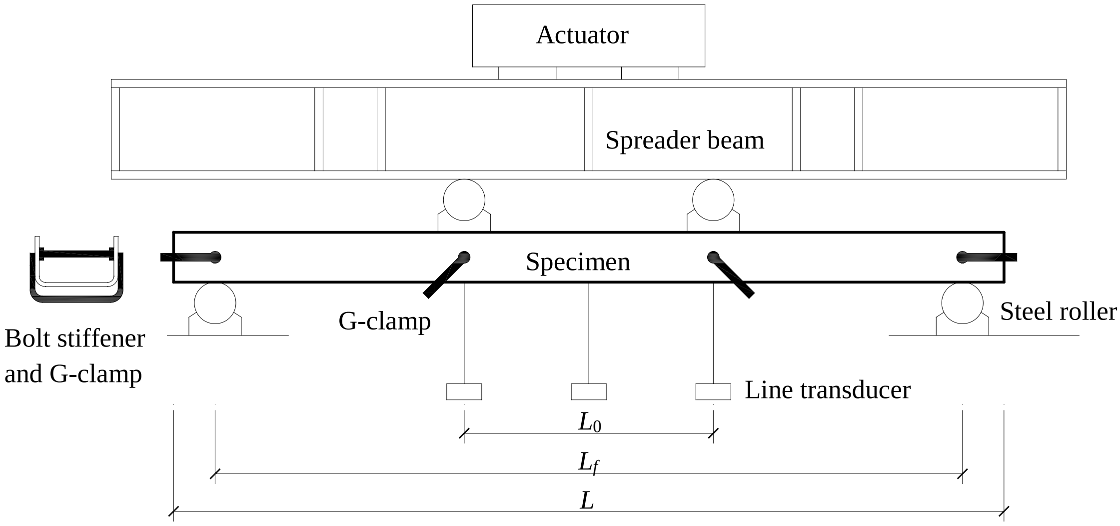

(b) Schematic diagram

Fig. 6. Experimental setup for press-braked S690 high strength steel channel section beams bent about the minor principal axes.

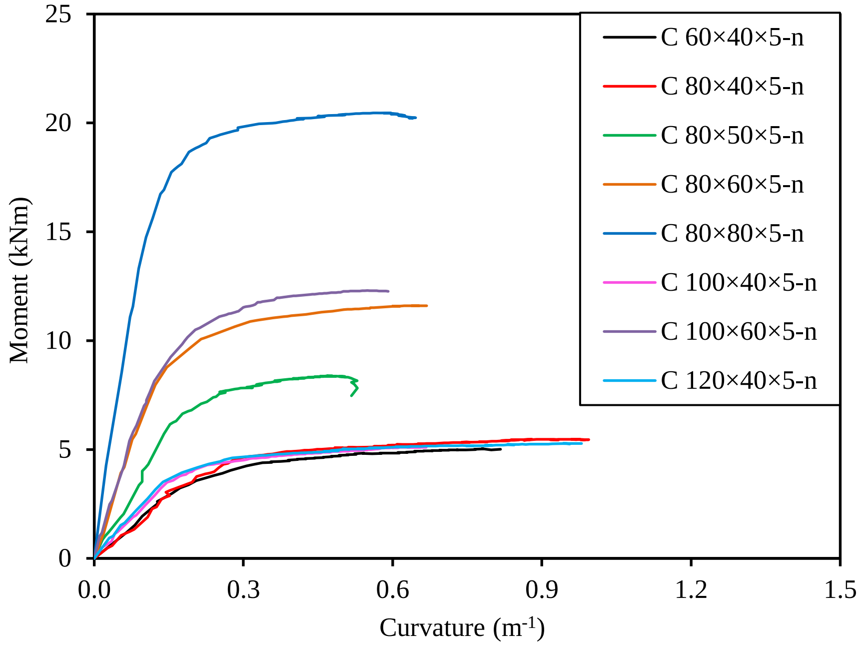

(a) Channel section beams bent in the ‘n’ orientation

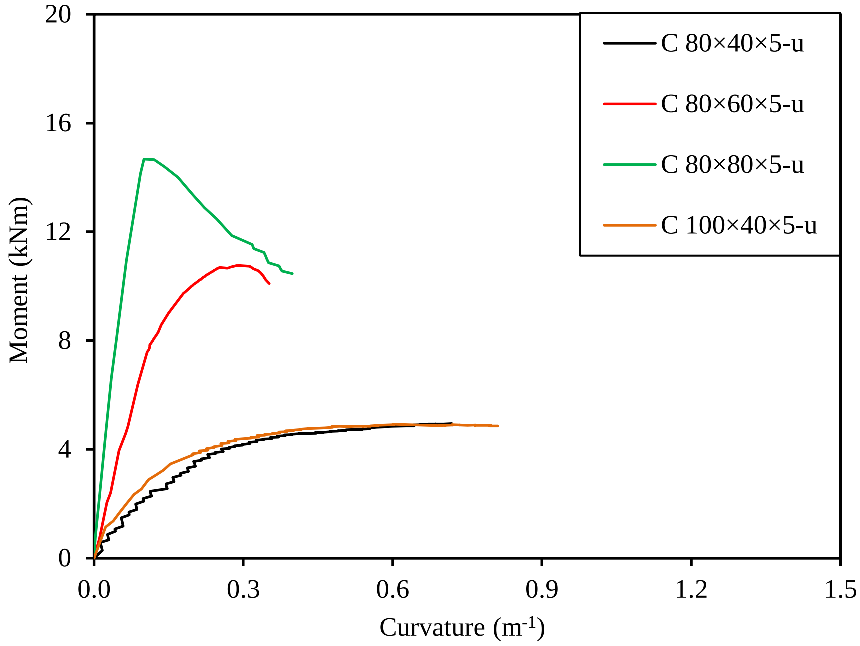

(b) Channel section beams bent in the ‘u’ orientation

Fig. 7. Moment–curvature curves of the tested press-braked S690 high strength steel channel section beam specimens.

Fig. 8. Experimental and numerical failure modes for press-braked S690 high strength steel channel section beam specimen C 80×60×5-n.

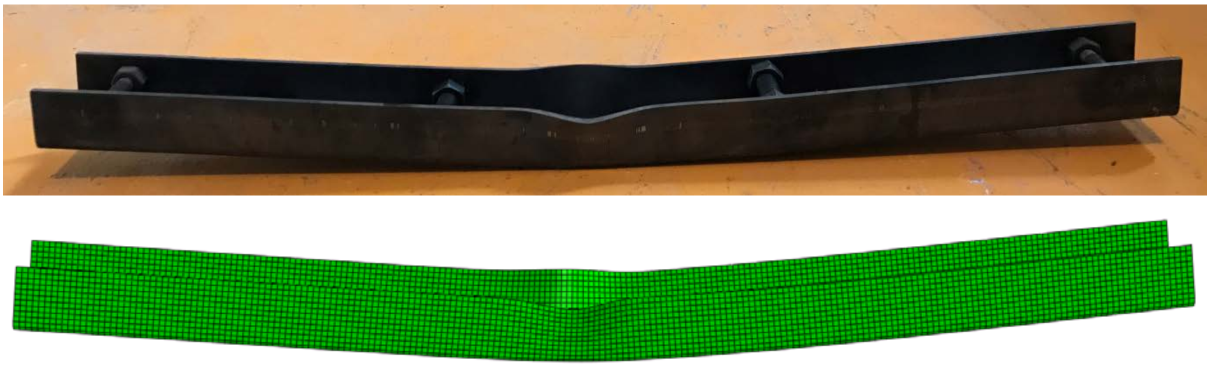

Fig. 9. Experimental and numerical failure modes for press-braked S690 high strength steel channel section beam specimen C 80×60×5-u.

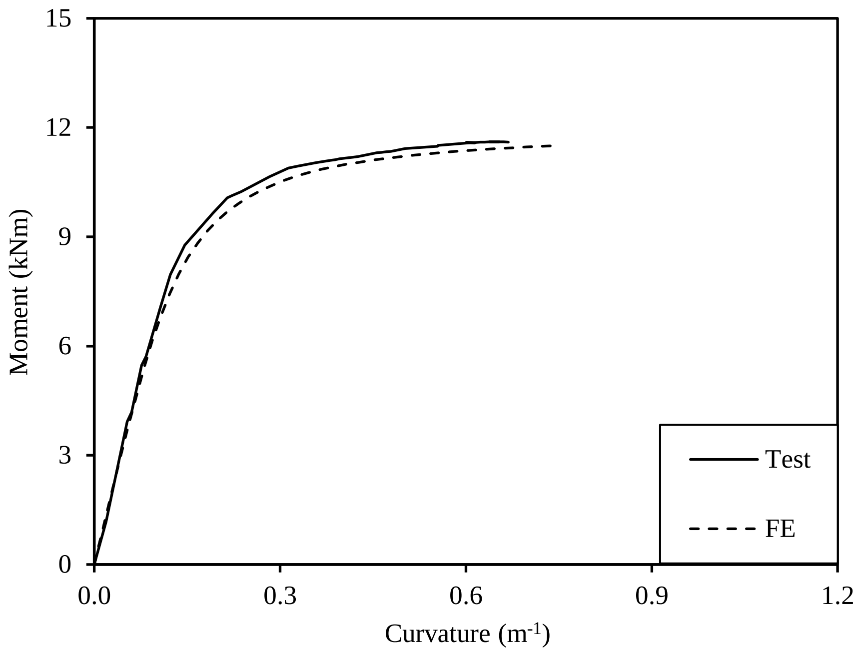

Fig. 10. Experimental and numerical moment–curvature curves for press-braked S690 high strength steel channel section beam specimen C 80×60×5-n.

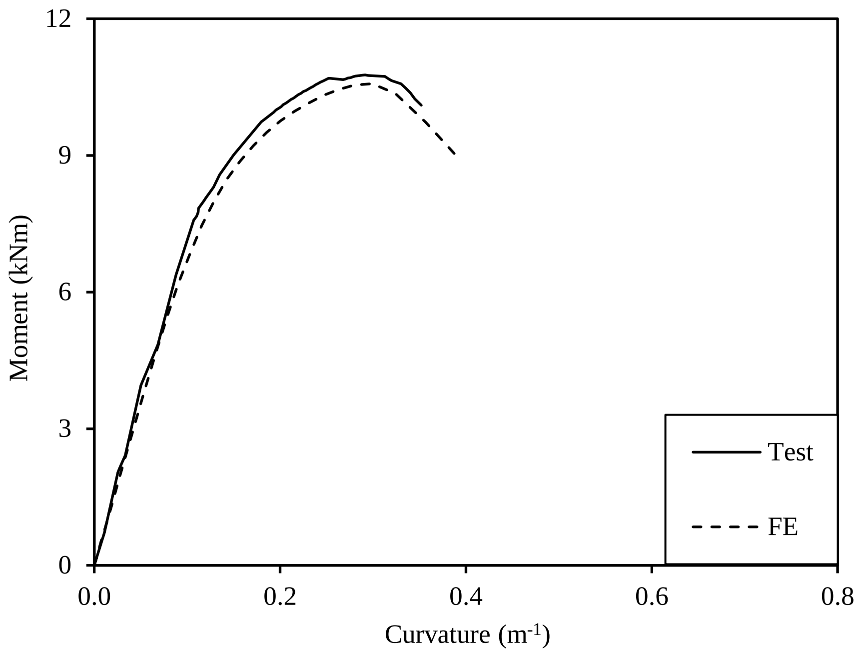

Fig. 11. Experimental and numerical moment–curvature curves for press-braked S690 high strength steel channel section beam specimen C 80×60×5-u.

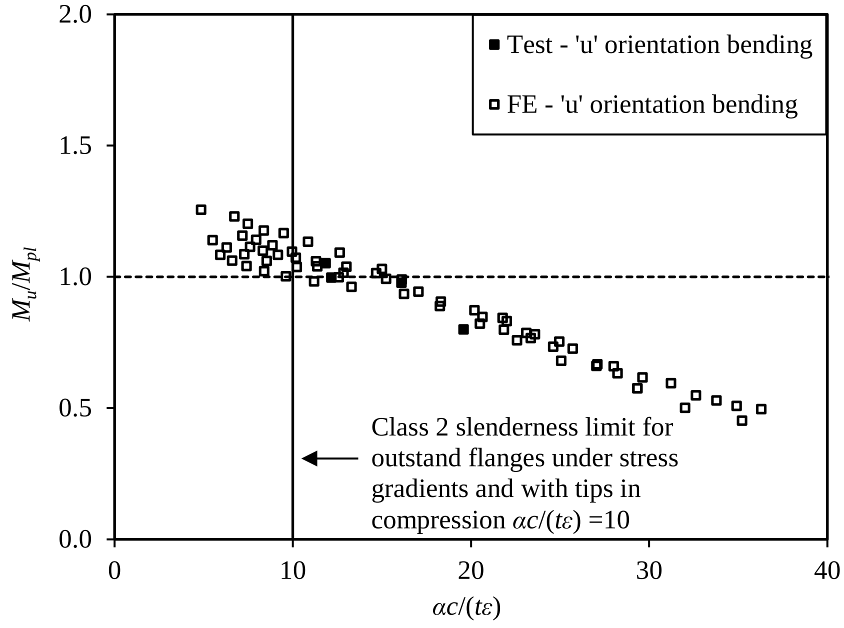

Fig. 12. Assessment of EC3 Class 2 slenderness limit for outstand flanges under stress gradients and with tips in compression.

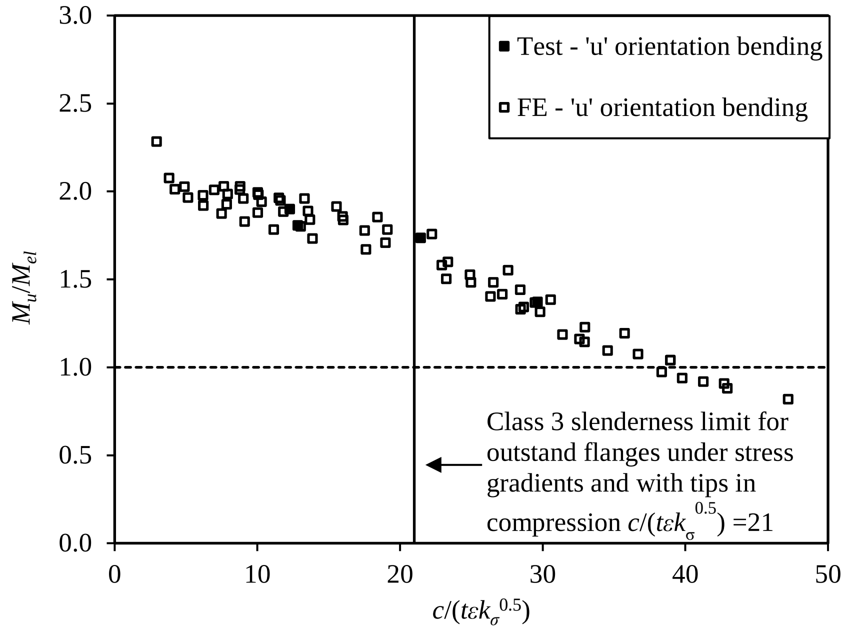

Fig. 13. Assessment of Class 3 slenderness limit for outstand flanges under stress gradients and with tips in compression.

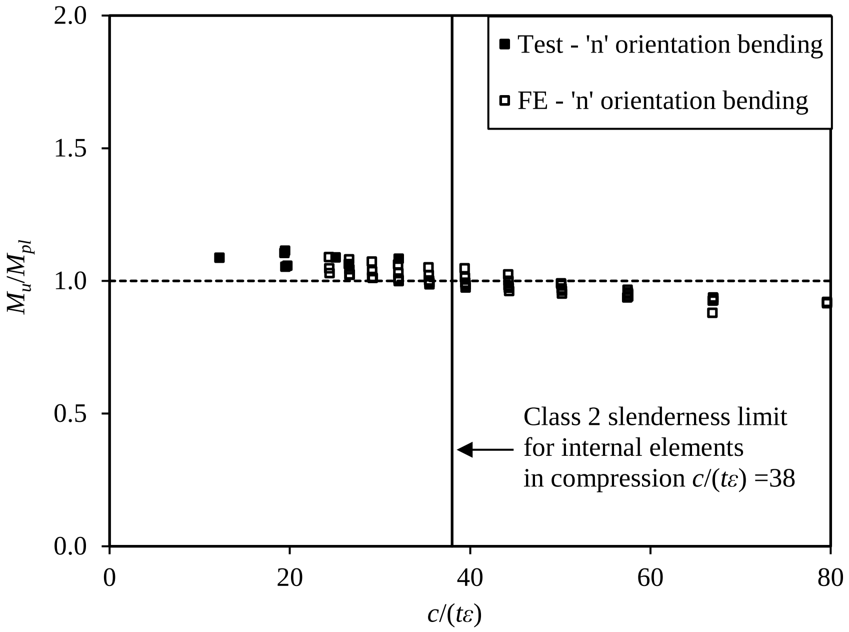

Fig. 14. Assessment of Class 2 slenderness limit for internal elements in compression.

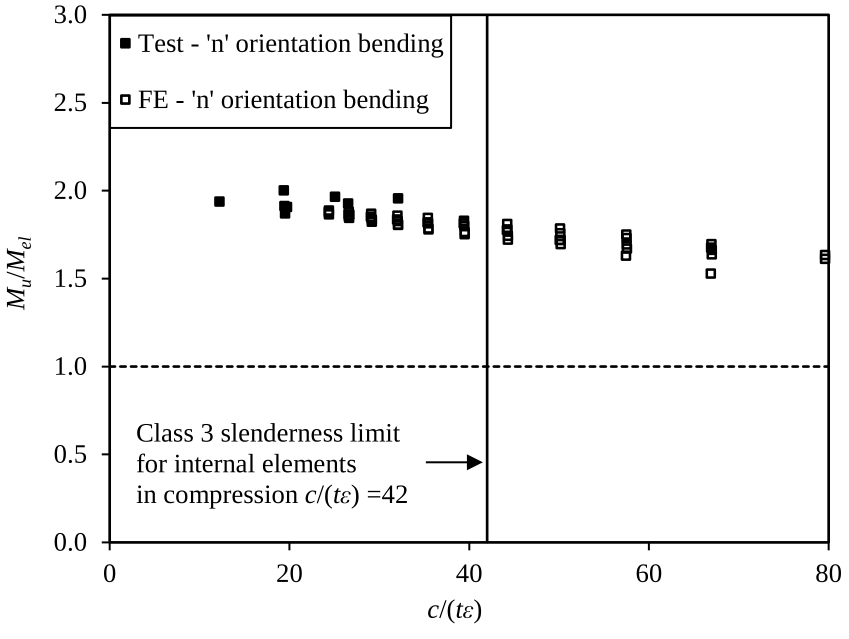

Fig. 15. Assessment of Class 3 slenderness limit for internal elements in compression.

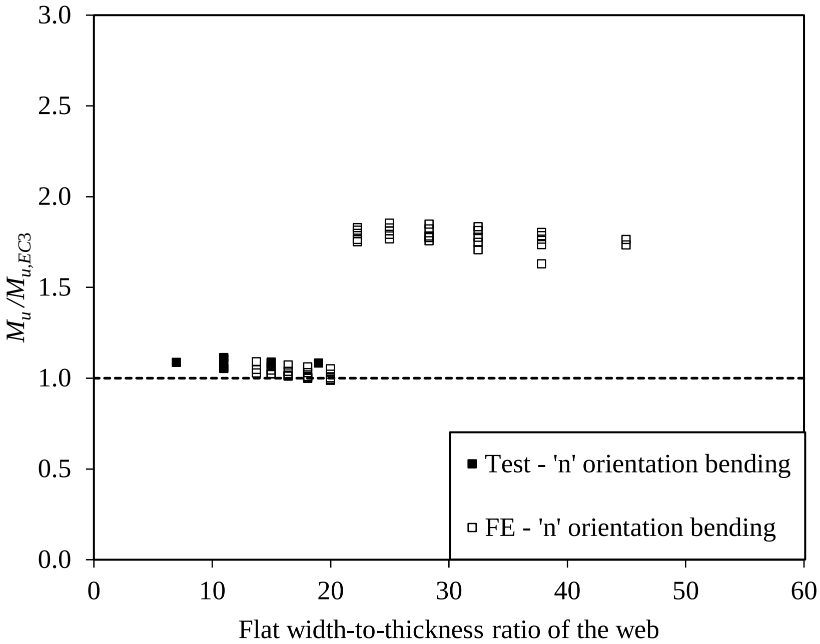

(a) Channel section beams bent in the ‘n’ orientation

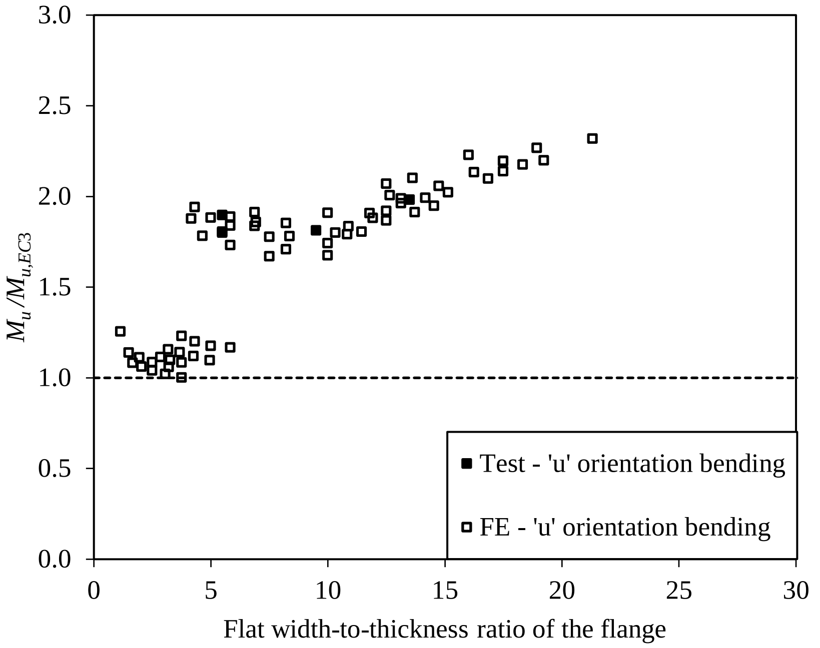

(b) Channel section beams bent in the ‘u’ orientation

Fig. 16. Comparisons of test and FE failure moments with EN 1993-1-12 flexural strength predictions.

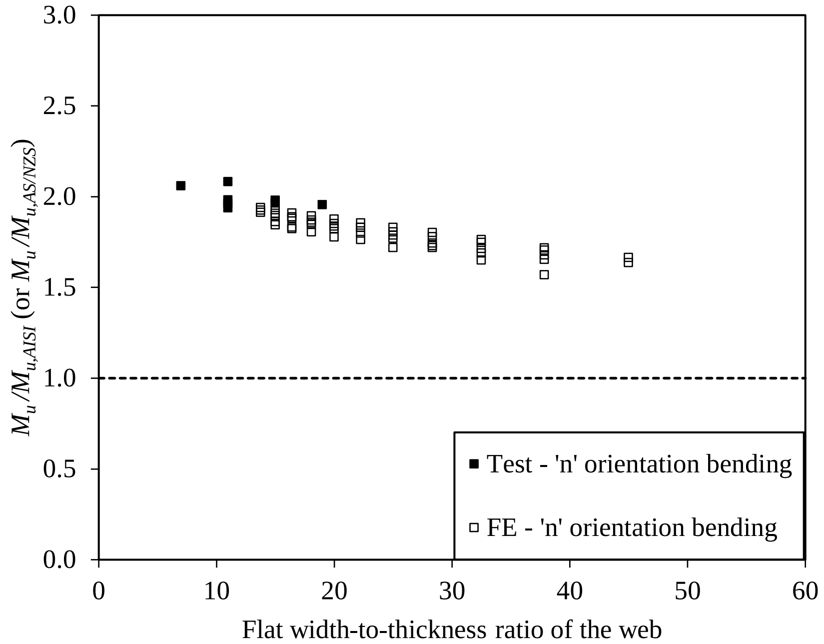

(a) Channel section beams bent in the ‘n’ orientation

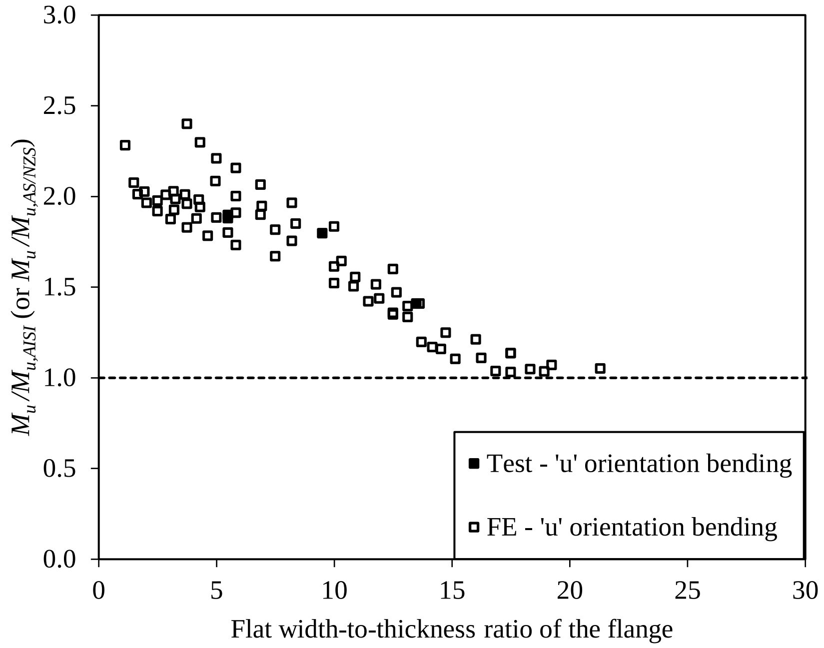

(b) Channel section beams bent in the ‘u’ orientation

Fig. 17. Comparisons of test and FE failure moments with AISI S100 (and AS/NZS 4600) flexural strength predictions.